

# 中国激光

## LD 端面抽运全固态声光调 Q 228.5 nm 深紫外激光器

赵志斌<sup>1,2</sup>, 陈浩<sup>2</sup>, 徐东昕<sup>2</sup>, 程成<sup>2</sup>, 李权<sup>2</sup>, 刘国军<sup>2</sup>, 乔忠良<sup>2</sup>, 孙丽<sup>2</sup>, 郑权<sup>3</sup>, 曲轶<sup>2\*\*</sup>, 薄报学<sup>1\*</sup>

<sup>1</sup>长春理工大学高功率半导体激光国家重点实验室, 吉林 长春 130022;

<sup>2</sup>海南师范大学物理与电子工程学院海南省激光技术与光电功能材料重点实验室, 海南 海口 571158;

<sup>3</sup>长春新产业光电技术有限公司, 吉林 长春 130103

**摘要** 采用三镜折叠 V 型谐振腔、声光调 Q 技术和三硼酸锂(LBO)晶体, 对二极管端面抽运 Nd: YVO<sub>4</sub> 的 914 nm 基频光进行腔内倍频, 实现了 457 nm 激光输出, 利用 I 类相位匹配偏硼酸钡(BBO)晶体对 457 nm 蓝光进行腔外倍频, 获得了 228.5 nm 深紫外激光。当抽运功率为 17 W 时, 获得了平均功率为 10 mW 的 228.5 nm 深紫外激光输出, 脉冲宽度为 64.26 ns, 重复频率为 10 kHz。2 h 内的激光输出稳定性为  $\pm 2\%$ 。

**关键词** 激光器; 全固态激光器; 声光调 Q 技术; 深紫外激光; 228.5 nm 激光

中图分类号 TN248.1 文献标志码 A

doi: 10.3788/CJL202249.0315001

深紫外激光在光谱分析、精密加工和激光医疗等领域都有重要的应用<sup>[1-5]</sup>。现阶段, 深紫外激光光源主要有准分子激光器、气体激光器、全固态激光器及利用同步加速器产生的同步辐射光源, 其中基于非线性频率转换的深紫外全固态激光器因其在效率、紧凑性和系统维护成本方面的优势而获得广泛关注<sup>[6-7]</sup>。本文主要研究用于拉曼光谱系统的紧凑型全固态深紫外激光光源。深紫外线的激发可以增强许多生物分子及一些爆炸物的拉曼强度<sup>[8-9]</sup>。最常规的获得深紫外全固态激光器的方法是对 Nd: YAG 的 1064 nm 谱线进行 4 倍频以得到 266 nm 激光。然而, 一些特殊的光谱应用需要一些特殊的深紫外波段。对于基于 Ti: sapphire 的激光器, 其 228 nm 附近波段的深紫外激光非常适用于检测基因组脱氧核糖核酸甲基化、蛋白质结构和爆炸物的拉曼光谱分析<sup>[10-13]</sup>。然而, Ti: sapphire 激光器系统复杂, 体积大。另外一种可能获得 228 nm 附近波段激光的方法是使用 Nd: YVO<sub>4</sub> 晶体的 914 nm 谱线产生 4 次谐波, 进而获得 228.5 nm 深

紫外激光。Nd: YVO<sub>4</sub> 作为激光晶体具有一些优势, 包括高的吸收横截面、宽的吸收带宽和偏振输出。虽然 Nd: YVO<sub>4</sub> 的导热性相对较差, 但由于热致屈光力是热导率的函数, Nd: YVO<sub>4</sub> 晶体内可产生一定的热透镜效应。在结构设计时, 考虑热透镜效应, 把 Nd: YVO<sub>4</sub> 晶体的泵浦面作为激光谐振腔的一个反射镜, 可使该激光器系统更简单、紧凑。目前, 已有利用 Nd: YVO<sub>4</sub> 晶体的 914 nm 谱线产生二次谐波以获得连续波 457 nm 激光的研究报道<sup>[14-15]</sup>。Nd: YVO<sub>4</sub> 晶体中的 914 nm 谱线是准三能级系统, 其受激发射截面比四能级系统小很多, 所以该波长的输出效率较低。为了增强其四倍频产生的 228.5 nm 深紫外激光输出, 需要对整个系统进行优化设计。本文采用三镜折叠 V 型腔和声光调 Q 技术, 对激光二极管(LD)抽运的 914 nm 基频光进行腔内二倍频, 产生了 457 nm 脉冲激光, 再通过腔外偏硼酸钡(BBO)晶体倍频, 获得了平均功率为 10 mW 的 228.5 nm 深紫外脉冲激光输出。

收稿日期: 2021-08-31; 修回日期: 2021-10-13; 录用日期: 2021-10-25

基金项目: 海南省重大科技计划(ZDKJ2019005)、海南省自然科学基金(618QN241, 2019RC169, 121QN228, 519MS051, 120MS031)、海南省科协青年科技英才创新计划(QCXM201810)、国家自然科学基金(61774024, 61864002, 61964007, 11764012)

通信作者: \*bbx@cust.edu.cn; \*\*quyihainan@126.com

实验装置如图 1 所示。采用的是 V 型谐振腔结构和激光脉冲运转方式,使基频光分臂获得合适的泵浦光与基频光的尺寸比,同时倍频光分臂中具有较小的光腰半径,从而提高 914 nm 基频光的倍频效率。从脉冲的稳定控制和系统简单方面考虑,调 Q 方式采用声光调制。抽运源采用光纤耦合输出的 808 nm 半导体激光器,其最大输出功率为 30 W,光纤芯径为 400  $\mu\text{m}$ ,数值孔径 NA = 0.22。耦合镜组由两个焦距为 10 mm 的平凸镜构成。抽运光经过准直聚焦系统后,抽运光光斑半径大约为 250  $\mu\text{m}$ 。Nd:YVO<sub>4</sub> 晶体中 Nd<sup>3+</sup> 的掺杂浓度(原子数分数)为 0.1%,尺寸为 4 mm × 4 mm × 5 mm,左端镀 808 nm、1064 nm 增透膜和 914 nm 高反膜,右端面镀 914 nm、1064 nm 和 1342 nm 增透膜。晶体采用 0.1 mm 厚的银箔包裹,被安装在紫铜热沉中,通过半导体制冷器(TEC)进行温度控制。曲率半径为 100 mm 的平凹镜 M 作为输出镜,凹面镀 914 nm 高反膜和 457 nm、1064 nm、1342 nm 增透膜,平面镀 457 nm、914 nm、1064 nm 和 1342 nm 增透膜;曲率半径为 200 mm 的平凹镜 M2 作为反射镜,表面镀 457 nm、914 nm 高反膜;Nd:YVO<sub>4</sub> 晶体的左端面 M1、M 和 M2 构成一个 V 型谐振腔,两臂夹角  $\alpha$  约为 5°。利用 ABCD 矩阵和稳定腔条件,考虑到 Nd:YVO<sub>4</sub> 的热效应以及抽运光与基频光之间的模式匹配,通过 Matlab 程序计算,臂 L1 和臂 L2 的长度分别取 160 mm 和 70 mm。其中长臂插入声光 Q 装置,短臂插入产生二次谐波的三硼酸锂(LBO)晶体并被放置在反射镜 M2 前约 1 mm 处。

LBO 采用 I 类临界相位匹配,由 SNLO 软件计算,尺寸为 4 mm × 4 mm × 15 mm 的 LBO 晶体的切割角度为  $\theta = 90^\circ$ ,  $\varphi = 21.7^\circ$ (在晶体的主轴坐标系中,  $\theta$  为波矢与光轴 Z 的夹角,  $\varphi$  为波矢在 YOZ 平面的投影与 X 轴的夹角),有效非线性系数为 0.803 pm/V, 914 nm 激光经 LBO 晶体倍频后, 457 nm 倍频光的走离角为 12.48 mrad, LBO 晶体两端面镀有 457 nm、914 nm 和 1064 nm 增透膜。M3 为 457 nm 聚焦镜, 表面镀有 457 nm 增透膜。根据最佳聚焦条件<sup>[16]</sup> 计算,M3 聚焦镜的焦距为 150 mm,BBO 晶体的尺寸 4 mm × 4 mm × 8 mm。由 SNLO 软件计算,采用 I 类临界相位匹配的 BBO 晶体的切割角为  $\theta = 61.4^\circ$ ,  $\varphi = 0^\circ$ , 有效非线性系数为 1.38 pm/V, 457 nm 激光经 BBO 晶体倍频后, 228.5 nm 倍频光的走离角为 75.68 mrad, BBO 晶体两端面镀有 457 nm 和 228.5 nm 增透膜。457 nm 激光从镜 M 射出, 经 M3 镜聚焦, 在焦点附近放置 BBO 晶体, 经 BBO 晶体倍频后即可产生 228.5 nm 深紫外激光, 并由分光棱镜 M4 分离出 457 nm 和 228.5 nm 激光。本实验采用美国 OCEAN OPTICS 公司的 HR4000CG-UV-NIR 光谱仪测量激光光谱, 利用加拿大 GENTEC-EO 公司的 MAESTRO 激光功率计测量激光输出平均功率, 利用美国 THORLABS 公司的 BP209/VIS 光束质量分析仪测量激光光斑, 利用美国 THORLABS 公司的 DET10A/M 探测器和美国 TEKTRONIX 公司的 TDS 3054C 示波器测量激光脉冲宽度。

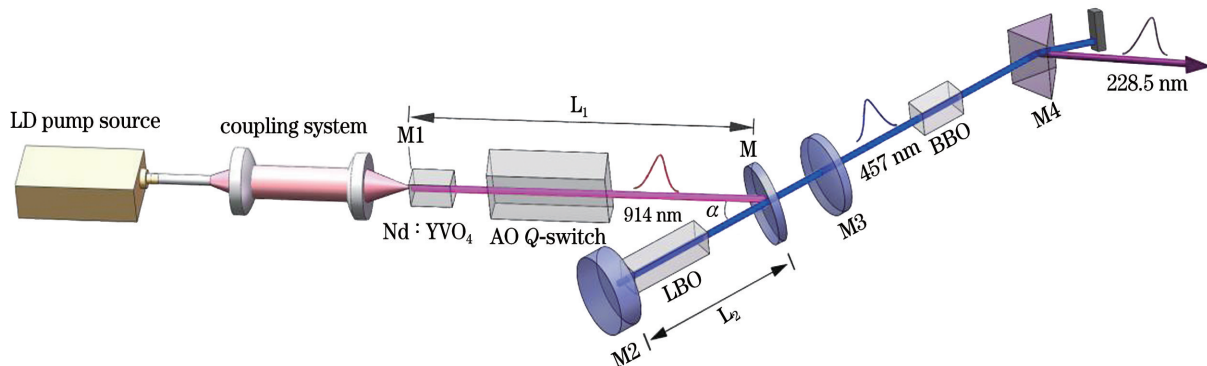


图 1 实验装置图

Fig. 1 Schematic of experimental setup

最终,在重复频率为 10 kHz、注入抽运功率为 17 W 条件下,获得了平均功率为 360 mW 的 457 nm 激光输出,脉冲宽度为 86 ns,光束质量 M<sup>2</sup> 因子为 1.12。经过 BBO 晶体后,得到了平均功率

为 10 mW 的 228.5 nm 深紫外激光,脉冲宽度为 64.26 ns。228.5 nm 激光的输出光谱、功率曲线、脉冲宽度和光斑图如图 2 所示。从图 2(a)得到,中心波长为 228.5 nm。从图 2(d)可以看出,228.5 nm

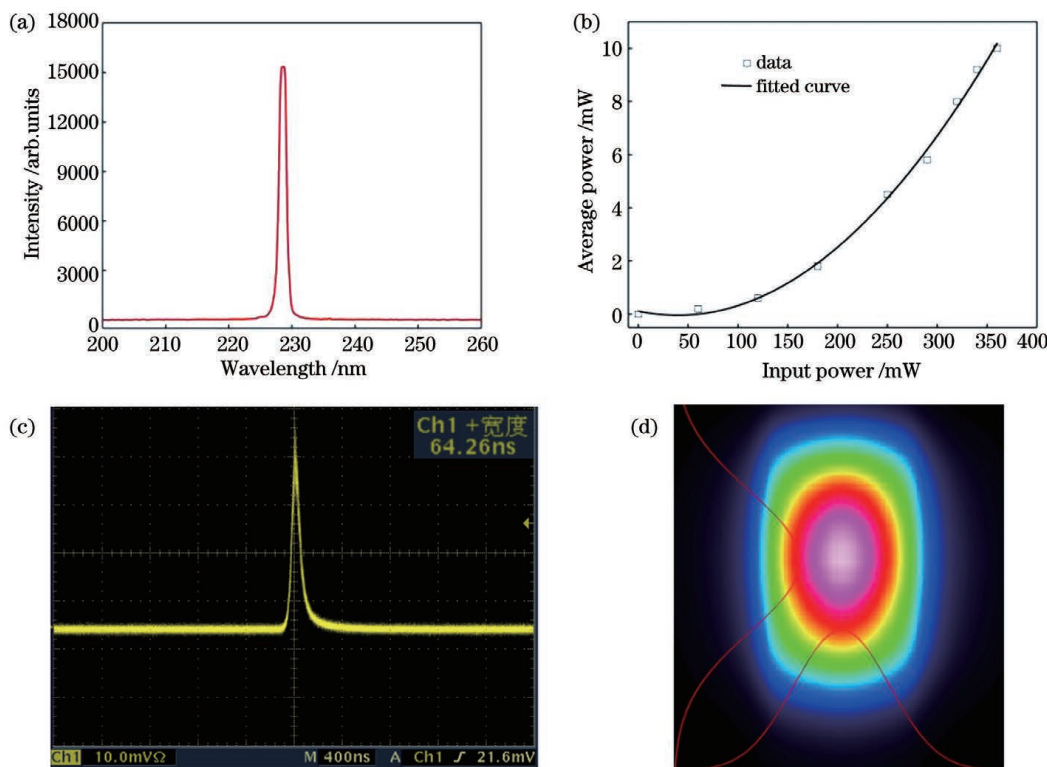


图 2 228.5 nm 深紫外激光的主要特征。(a)光谱;(b)功率曲线;(c)脉冲宽度;(d)光斑

Fig. 2 Main characteristics of 228.5 nm deep ultraviolet laser. (a) Spectrum; (b) power curve; (c) pulse duration; (d) spot

激光输出光斑为椭圆形,原因是 457 nm 激光经 BBO 晶体倍频后,228.5 nm 倍频光的走离角较大。

## 参 考 文 献

- [1] Shao F, Wang W, Yang W M, et al. *In-situ* nanospectroscopic imaging of plasmon-induced two-dimensional [4 + 4]-cycloaddition polymerization on Au(111) [J]. *Nature Communications*, 2021, 12: 4557.
- [2] Zhao Y, Xiang Y, Li T T. Optical design of deep ultraviolet laser irradiation system for accelerating material aging[J]. *Acta Optica Sinica*, 2021, 41(5): 0522001.  
赵阳, 向阳, 李婷婷. 深紫外激光辐照加速材料老化系统的光学设计 [J]. 光学学报, 2021, 41(5): 0522001.
- [3] Qi Y F, Liu Y H, Liu D M. Research progress on application of Raman spectroscopy in tumor diagnosis [J]. *Laser & Optoelectronics Progress*, 2020, 57(22): 220001.  
祁亚峰, 刘宇宏, 刘大猛. 拉曼光谱技术在肿瘤诊断上的应用研究进展 [J]. 激光与光电子学进展, 2020, 57(22): 220001.
- [4] Zheng J Q, Cong Z H, Liu Z J, et al. Recent trend of high repetition rate ultrashort laser pulse generation and frequency conversion [J]. *Chinese Journal of Lasers*, 2021, 48(12): 1201008.  
郑佳琪, 丛振华, 刘兆军, 等. 高重复频率超短激光脉冲产生及频率变换技术发展趋势 [J]. 中国激光, 2021, 48(12): 1201008.
- [5] Wang J Y, Li Q, Chen X, et al. A high-frequency all-solid-state ultraviolet laser at 244 nm[J]. *Chinese Journal of Lasers*, 2019, 46(9): 0901010.  
王金艳, 李奇, 陈曦, 等. 全固态高重复频率 244 nm 紫外激光器 [J]. 中国激光, 2019, 46(9): 0901010.
- [6] Hsiao R L, Chen Y C, Huang M Y, et al. Innovative finding of 266-nm laser regulating CD90 levels in SDSCs[J]. *Scientific Reports*, 2021, 11(1): 13932.
- [7] Zhang B T, Liu J, Wang C, et al. Recent progress in 2D material-based saturable absorbers for all solid-state pulsed bulk lasers [J]. *Laser & Photonics Reviews*, 2020, 14(2): 1900240.
- [8] Kumamoto Y, Taguchi A, Kawata S. Deep-ultraviolet biomolecular imaging and analysis [J]. *Advanced Optical Materials*, 2019, 7(5): 1801099.
- [9] Zrimsek A B, Bykov S V, Asher S A. Deep ultraviolet standoff photoacoustic spectroscopy of trace explosives[J]. *Applied Spectroscopy*, 2019, 73(6): 601-609.
- [10] D'Amico F, Zucchiatti P, Latella K, et al. Investigation of genomic DNA methylation by

- ultraviolet resonant Raman spectroscopy[J]. Journal of Biophotonics, 2020, 13(12): e202000150.
- [11] Asamoto D K, Kim J E. UV resonance Raman spectroscopy as a tool to probe membrane protein structure and dynamics [M] // Kleinschmidt J H. Lipid-protein interactions. Methods in molecular biology. New York: Humana, 2019, 2003: 327-349.
- [12] Leigh B S, Monson K L, Kim J E. Visible and UV resonance Raman spectroscopy of the peroxide-based explosive HMTD and its photoproducts[J]. Forensic Chemistry, 2016, 2: 22-28.
- [13] Shafaat H S, Sanchez K M, Neary T J, et al. Ultraviolet resonance Raman spectroscopy of a  $\beta$ -sheet peptide: a model for membrane protein folding [J]. Journal of Raman Spectroscopy, 2009, 40(8): 1060-1064.
- [14] Xue Q H, Zheng Q, Bu Y K, et al. High-power efficient diode-pumped Nd: YVO<sub>4</sub>/LiB<sub>3</sub>O<sub>5</sub> 457 nm blue laser with 4.6 W of output power[J]. Optics Letters, 2006, 31(8): 1070-1072.
- [15] Yin H, Zhu S Q, Chen Z Q, et al. Research on all-solid-state intracavity frequency doubling 457 nm laser with LBO and BIBO crystal[J]. Optik, 2016, 127(8): 3862-3866.
- [16] Boyd G D, Kleinman D A. Parametric interaction of focused Gaussian light beams[J]. Journal of Applied Physics, 1968, 39(8): 3597-3639.

## LD End-Pumped All-Solid-State Acousto-Optical Q-Switched 228.5 nm Deep Ultraviolet Laser

Zhao Zhibin<sup>1,2</sup>, Chen Hao<sup>2</sup>, Xu Dongxin<sup>2</sup>, Cheng Cheng<sup>2</sup>, Li Quan<sup>2</sup>, Liu Guojun<sup>2</sup>, Qiao Zhongliang<sup>2</sup>, Sun Li<sup>2</sup>, Zheng Quan<sup>3</sup>, Qu Yi<sup>2\*</sup>, Bo Baoxue<sup>1\*</sup>

<sup>1</sup> State Key Laboratory of High Power Semiconductor Laser, Changchun University of Science and Technology, Changchun, Jilin, 130022, China;

<sup>2</sup> Key Laboratory of Laser Technology and Optoelectronic Functional Materials of Hainan Province, College of Physics and Electronic Engineering, Hainan Normal University, Haikou, Hainan 571158, China;

<sup>3</sup> Changchun New Industries Optoelectronics Technology Co., Ltd., Changchun, Jilin, 130103, China

### Abstract

**Objective** Deep ultraviolet (DUV) lasers have an important and irreplaceable role in the field of spectral analysis. At present, DUV laser sources are mainly excimer lasers, gas lasers, solid-state lasers or those generated by synchrotron radiation. Deep ultraviolet all-solid-state lasers based on nonlinear frequency conversion have gained great popularity because of its compact, low system maintenance cost, and high efficiency. The most common approach is the fourth-harmonic generation of the 1064 nm laser line of Nd:YAG, which has been a commercial product for many years. Unfortunately, some particular spectroscopic applications require specific wavelengths in the DUV region. Based on Ti: Sapphire lasers, those with output power of several mW in the vicinity of 228 nm deep ultraviolet region have proved very suitable in the detection of genomic deoxyribonucleic acid methylation, protein structure, and explosive Raman spectroscopic analysis. However, Ti: Sapphire laser systems are complex, bulky, and inefficient. This paper introduces a new compact 228.5 nm high-repetition-rate, frequency-quadrupled Nd:YVO<sub>4</sub> laser as a new excitation source for ultraviolet resonance Raman spectroscopic analysis.

**Methods** Figure 1 shows the experimental principle. Via a V-shaped folded-cavity, the acousto-optical Q-switched technology and a LiB<sub>3</sub>O<sub>5</sub> (LBO) crystal, the 914 nm fundamental laser has been obtained by laser diode (LD) end-pumping, which is then used for intra-cavity frequency doubling generation of a pulsed 457 nm laser. This blue laser is frequency-converted to a 228.5 nm laser in a  $\beta$ -BaB<sub>2</sub>O<sub>4</sub> (BBO) crystal. The pump source is a 30 W 808 nm fiber-coupled LD with a core diameter of 400  $\mu$ m and a numerical aperture of 0.22. The coupling system is composed of two plano-convex mirrors with a focal length of 10 mm. The pumping light is focused and collimated into a light beam of about 250  $\mu$ m in radius through the collimation and focusing system. A Nd:YVO<sub>4</sub> crystal with a doping concentration (atomic fraction) of 0.1% and a dimension of 4 mm  $\times$  4 mm  $\times$  5 mm is employed as the gain medium. The left facet is antireflection coated at 808 nm and 1064 nm and high-reflection coated at 914 nm, and the right facet is antireflection coated at 914, 1064, and 1342 nm wavelengths. The laser crystal is wrapped in a layer of

indium foil on the side and secured on a copper heat sink, which is capable of controlling the temperature through circulating water cooling. The radii of the concave mirrors M and M2 are 100 mm and 200 mm, respectively. The V-shaped cavity is formed by the left facet of Nd:YVO<sub>4</sub> crystal (M1) and M2, where the angle between two arms is about 5°. Using the ABCD matrix and stable cavity conditions, considering the thermal effect of Nd:YVO<sub>4</sub> and the mode matching between pumping light and fundamental frequency light, and through numerical calculation by Matlab programming, one can obtain that the lengths of L1 and L2 are 160 mm and 70 mm, respectively. The 15 mm long LBO crystal is cut for the type-I critical-phase-matching condition ( $\theta = 90^\circ$ ,  $\varphi = 21.7^\circ$ ), and both facets are antireflection coated at 457 nm, 914 nm, and 1064 nm. The 8 mm long BBO crystal is cut for the type-I critical-phase-matching condition ( $\theta = 61.4^\circ$ ,  $\varphi = 0^\circ$ ). Both facets of the BBO crystal are antireflection coated at 457 nm and 228.5 nm.

**Results and Discussions** At a pump power of 17 W and a repetition rate of 10 kHz, the mean output power for the 457 nm laser has reached 360 mW at an 86 ns pulse duration. With the type-I phase-matched BBO crystal, the externally frequency doubling of a 457 nm blue output is realized, and the 228.5 nm DUV laser has been achieved with a mean output power of 10 mW at repetition rate of 10 kHz and pulse duration of 64.26 ns [Figs. 2(b) and 2(c)]. The 228.5 nm laser spot is shown in Fig. 2(d), with a somewhat elliptic shape as the result of the walk-off effect.

**Conclusions** A compact all-solid-state DUV-laser source producing a short pulse at 228.5 nm is reported. The acoustically Q-switched quasi-three-level Nd:YVO<sub>4</sub> laser at 914 nm is first intra-cavity frequency doubled into a blue laser with an LBO nonlinear crystal, and then into a DUV output from externally frequency doubling of the blue laser with a BBO nonlinear crystal. The 228.5 nm DUV pulsed laser output power of 10 mW is obtained, with a stable output power and good output beam quality. The present laser system is simple, compact and portable compared with the Ti: sapphire UV Raman laser reported earlier. Our laser source can be favorably used in the spectroscopic measurement of explosives and biomolecules.

**Key words** lasers; all-solid-state lasers; acousto-optical Q-switching technology; deep ultraviolet laser; 228.5 nm laser